NaK Λ doubling and permanent electric dipoles in low-lying $^1\Pi$ states: Experiment and theory

M. Tamanis, M. Auzinsh, I. Klincare, O. Nikolayeva, and R. Ferber
Department of Physics, University of Latvia, Riga LV-1586, Latvia

E. A. Pazyuk, A. V. Stolyarov, and A. Zaitsevskii
Department of Chemistry, Moscow M. Lomonosov State University, Moscow 119899, Russia

(Received 23 December 1997)

The paper presents Λ splittings and q factors in the NaK $D\ ^1\Pi$ state, directly measured from the electric radio-frequency-optical double resonance (RF-ODR) in laser-induced fluorescence (LIF) for a number of vibrational states $v=1-22$ with definite rotational levels J between 7 and 46. Permanent electric dipole moment values (d) have been obtained by measuring in LIF spectra the relative intensities of ''forbidden'' lines caused by dc Stark effect induced e/f mixing in the $^1\Pi$ state, with their subsequent processing, which allowed us to obtain the q/d ratio. A possible influence of the hyperfine structure on the RF-ODR signal and relative intensities has been calculated, showing that this influence can be neglected. The $q(v)$ values exhibited a decrease from $q(1)=1.529\times10^{-5}$ cm^{-1} to $q(22)=1.171\times10^{-5}$ cm^{-1}, which has been explained by an increase of the difference potential between $D\ ^1\Pi$ and $C\ ^1\Sigma^+$ states with internuclear distance (R); the respective L-uncoupling matrix element was evaluated as 1.87. It was shown, both by semiempirical treatment and population analysis of *ab initio* molecular wave functions, that considerable πd and σd configuration admixtures are present in the $D\ ^1\Pi$ and the $C\ ^1\Sigma^+$ states. For the $B\ ^1\Pi$ state, it was demonstrated that Λ doubling is caused by two competing perturbers ($A\ ^1\Sigma^+$ and $C\ ^1\Sigma^+$), yielding q factors of $\sim-2\times10^{-6}$ cm^{-1}, in agreement with high-resolution spectroscopy data given in the literature; single-configuration approximation is valid for interacting $B\ ^1\Pi(\sigma 3s_{\mathrm{Na}},\pi 4p_{\mathrm{K}})\sim A\ ^1\Sigma^+(\sigma 3s_{\mathrm{Na}},\sigma 4p_{\mathrm{K}})$ states. The measured $d(v)$ values, which varied from 6.6 to 4.6 D, have been used to obtain the empirical $D\ ^1\Pi$ state $d(R)$ function for $R=6-12$ a.u. by means of an improved instability-free inversion procedure exploiting a special functional form. Two independent series of *ab initio* all-electron calculations of $d(R)$ and $d(v)$ have been performed for the $D\ ^1\Pi$ and $B\ ^1\Pi$ states of NaK. First, d values were computed as expectation values of the electric dipole operator with conventional multireference configuration-interaction wave functions. Second, the finite-field (FF) technique, combined with a multipartitioning perturbation theory (MPPT) treatment of electronic eigenstates, was applied for the calculation of $d(R)$ functions. The FF-MPPT calculations showed excellent agreement with experimental $D\ ^1\Pi$ $d(v)$ values obtained in the present work, as well as the proximity to experimental $B\ ^1\Pi$ $d(v)$ values given in the literature, thus showing that, as distinct from the ground state, it is important to account correctly for effective interactions of valence electrons arising from core-valence correlations, which could not be done properly with previously used pseudopotential techniques. The experimental d and q values dropping out from a smooth v dependence have been considered as perturbed by $D\ ^1\Pi\sim d\ ^3\Pi$ interaction and exploited to evaluate respective d_t and c_t values for the perturbing $d\ ^3\Pi$ state. [S1050-2947(98)11309-4]

PACS number(s): 33.15.−e, 31.15.−p

I. INTRODUCTION

Experimental determination of the permanent electric dipole moment (PEDM) in diatomic molecules is of great interest for the following reasons. First, the dipole moment gives direct information about charge distribution in the particular molecular state, as well as about the type of binding. Besides, the PEDM value enters the expressions describing the intensities of microwave transitions between the levels belonging to the same electronic molecular states. Next, the PEDM is extremely sensitive to the details of the electronic wave function (WF), hence an accurate experimental knowledge of this quantity is very useful as a test allowing us to judge to what extent the *ab initio* calculations of WF's are reliable.

Though there exists considerably rich information on experimentally measured electronic $^1\Sigma^+$ ground-state electric dipole moments of small molecules, see, e.g., [1], the situation is different for electronically excited states. Speaking about the heteronuclear alkali-metal diatomic molecules, one has to admit that even for NaK, which is the most closely studied molecule of this class, there still exist more questions than answers. The first results have been reported on NaK PEDM measurements in the $B\ ^1\Pi$ [2] and $D\ ^1\Pi$ [3] electronic states, while their *ab initio* pseudopotential calculations are presented in [4]. In particular, in our previous paper [3] the PEDM $d^{\mathrm{exper}}(D\ ^1\Pi)$ values have been determined for two rovibronic levels $v(J)$ as 5.9–6.4 D for 7(23) and 4.5–4.8 D for 12(7). From another point, theoretical methods that would permit us to calculate, with sufficiently high accuracy, the excited state PEDM are still questionable. The ground $X\ ^1\Sigma^+$ state PEDM's calculated in the vicinity of the minimum of the potential curve using the effective core potential (or pseudopotential) methods by Müller and Meyer [5] as 2.735 D, by Stevens and co-authors [4] as 2.95 D, and by Magnier and Millie [6] as 2.758 D, are in excellent agree-

ment with the experimental value $d^{\text{exper}}(X\ ^1\Sigma^+)=2.73$ D [7]. Yet, it is still not clear enough whether the above approaches allow us to obtain reliable results to describe excited state dipole moments. The authors of Ref. [2] have found large discrepancies between their measured $d^{\text{exper}}(B\ ^1\Pi)=(2.4-2.1)$ D values for v ranging from 1 to 14, and the PEDM's calculated in Ref. [4] as (4.5–2.8) D. Calculations [4] for NaK $D\ ^1\Pi$ also exhibit some tendency to exceed the above experimental $d^{\text{exper}}(D\ ^1\Pi)$ evaluations [3]. It is probably worth mentioning that an attempt has been made [8] to study the PEDM of NaK by the *ab initio* internally contracted configuration-interaction (CI) method using the MOLPRO package [9]. While for the *ab initio* calculated value for NaK $X\ ^1\Sigma^+$ $d(R_e)=2.79$ D is quite good, the ~9 D value obtained for the NaK $D\ ^1\Pi$ state is much above the experimental value of 5–6 D [3]. For a definite conclusion, more experimental data are needed, in particular, those allowing us to obtain the experimental $d(R)$ dependence within a somewhat considerable R range.

A peculiarity of spectroscopic investigations of $^1\Pi$ states is that such states possess Λ splitting into two *e,f* components within each vibronic level $v(J)$. In the simplest case Λ splitting Δ_{ef} is characterized by a so-called q factor [10,11]

$$\Delta_{e,f}=E_e-E_f=qJ(J+1). \tag{1}$$

It is quite obvious that, especially for large J values, highly accurate q_{vJ} values are necessary to have a reliable set of molecular constants: without such data it is hopeless to reproduce the $^1\Pi(v,J)$ state energy. On the other hand, the q values reflect directly the measure of intramolecular $^1\Pi \sim ^1\Sigma$ interaction, yielding an essentially novel insight into the structure not only of an isolated $^1\Pi$ state, but of a $^1\Pi \sim ^1\Sigma$ complex and, to some extent, of a $^1\Pi \sim ^3\Pi$ complex as well. The existing information about Λ doubling in alkali-metal dimers is far from sufficient also for the NaK molecule, which has been the subject of intensive spectroscopic studies [2,3,12–15]. In particular, some contradictions have been revealed for the NaK $B\ ^1\Pi$ state between the q values measured from line positions in optical spectra [15] and from Stark effect based methods [2]. For the NaK $D\ ^1\Pi$ state under study in the present paper, there is also a discrepancy between the average q value of the order of 1.16×10^{-5} cm^{-1}, as obtained from conventional spectroscopic analysis for high $J>70$ [12] and the value 1.42×10^{-5} cm^{-1} measured in Ref. [3] for $v(J)=7(23)$. In the case of the NaK molecule, it can be expected that the comparison between experimental and theoretical q values might allow us to judge to what extent the simple single configurational $4s_{\text{K}}+3p_{\text{Na}}$ approximation of the $D\ ^1\Pi$ state is correct.

The purpose of the present work is to elaborate the methods developed in [3] and to apply them to get more accurate experimental d and q values within a wide range of NaK $D\ ^1\Pi$ state vibrational levels, as well as to perform high accuracy *ab initio* $d(R)$ calculations, and to check their reliability by comparison with experimentally obtained data.

The rest of this paper runs as follows. In the next section we describe briefly the basis of the method, experimental details, and the signal processing routine. Section III contains the obtained experimental data. The polynomial approximation of the q factor data, as well as their semiempirical estimations, are presented in Sec. IV. Section V contains the description of the inversion procedure allowing to pass from experimentally obtained $d(v,J)$ values to $d(R)$ functions for the $D\ ^1\Pi$ and $B\ ^1\Pi$ states of the NaK molecule. The *ab initio* PEDM calculation is described in Sec. VI, followed by a discussion on the influence of $d\ ^3\Pi \sim D\ ^1\Pi$ mixing upon dipole moments and q factors in Sec. VII, and concluding remarks in Sec. VIII.

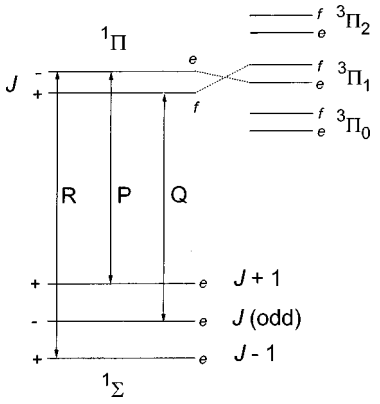

FIG. 1. Λ-doubling scheme and selection rules for optical transitions.

II. METHOD

A. Basic considerations

The idea of the method is very simple; see Fig. 1, cf. [2,3,16–18]. Focusing on diatomics in $^1\Pi$ singlet states, one faces the necessity of distinguishing between the two Λ-doublet states of a rotating molecule. The electronic-rotational WF $|\Lambda JM\epsilon\rangle$ can be expressed as a linear combination over rotational $|\Lambda JM\rangle$ parts [10,19,20]:

$$|\Lambda JM\epsilon\rangle=\frac{1}{\sqrt{2}}\left(|\Lambda\rangle|\Lambda JM\rangle+\epsilon|-\Lambda\rangle|-\Lambda JM\rangle\right), \tag{2}$$

$\epsilon=\pm1$ being the ''parity index'' distinguishing between the two Λ-doublet states possessing total parity $+(-1)^J$ for $\epsilon=+1$ (labeled as *e*), and $-(-1)^J$ for $\epsilon=-1$ (labeled as *f*), $\Lambda=|\Lambda|$. The two Λ-doublet states are degenerate in the first order with respect to their energy. Thus, the energy splitting $\Delta_{e,f}$ in Eq. (1) appears as a perturbation of a $^1\Pi$ state. Most frequently the dominating perturbation is caused by the fact that the rotationally induced $^1\Pi$ state interaction with a $^1\Sigma$ state can take place only for one of the $\epsilon=\pm1$ components. In most cases one member of a Λ-doublet pair (*e* or *f*) has a preferred population both in optical excitation [due to the $(+)\leftrightarrow(-)$ total parity selection rules [10,21]; see Fig. 1], as well as in chemical reactions and inelastic collisions. Owing to the same selection rule, the $^1\Pi-^1\Sigma$ fluorescence spectrum consists either of singlets following Q excitation or of doublets following P,R excitation; see Fig. 1. In the presence of a dc electric field, *e* and *f* levels are mixed via the Stark interaction operator $\mathbf{d}\boldsymbol{\mathcal{E}}$, $\boldsymbol{\mathcal{E}}$ being the dc electric field strength. This leads to the appearance of ''forbidden'' lines in the fluorescence spectra, in which one can now observe the whole P,Q,R triplet. The intensity of the ''forbidden'' line (I_f) is ''borrowed'' from the ''allowed'' lines, and the $\mathcal{E}$

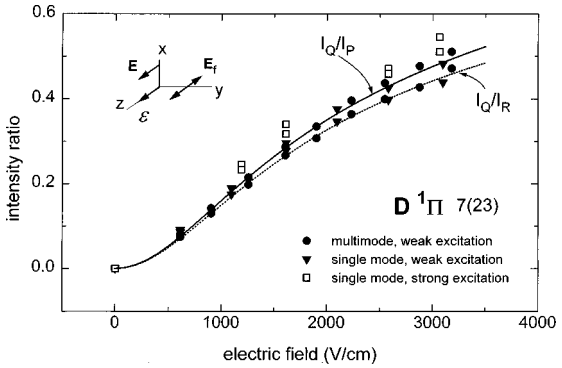

FIG. 2. Experimentally obtained I_f/I_p intensity ratios for LIF progression originating from NaK $D\ ^1\Pi\ v(J)=7(23)$ level. $\mathbf{E}$,$\mathbf{E_f}$ denote exciting light and LIF electric vectors, $\mathcal{E}$ being external electric field.

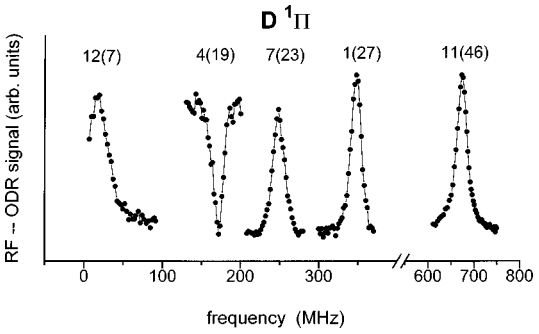

FIG. 3. Experimentally obtained RF-ODR signals for various $v(J)$ $D\ ^1\Pi$ levels.

dependence of the ratio I_f/I_p, see Fig. 2, I_p being the ''parent'' line intensity, allows us, by proper fitting described in detail in Ref. [3], to obtain the ratio Δ_{ef}/d.

In the case when a radio-frequency (RF) electric field is applied, in resonance with *e,f* splitting $\Delta_{e,f}$, the appearance of a ''forbidden'' line is also expected in the laser-induced fluorescence (LIF) spectrum. This means that, if the spectral apparatus is tuned to the ''forbidden'' line position, one will be able to detect, against zero background, even the slightest appearance of the missing line in a situation when the scanned RF electric field frequency equals $\Delta_{e,f}/h$; see Fig. 3. This permits us to measure Δ_{ef} directly and to pass to the q factors; see Eq. (1). On the other hand, it is also possible to use the resonant diminution of the allowed transition intensity I_p (Fig. 3) for the same purpose. Thus, by combining the electric RF–optical double resonance (RF-ODR) method [22] yielding Δ_{ef} with the dc Stark effect induced $e\sim f$ mixing yielding Δ_{ef}/d, one obtains the d values desired.

B. Experimental details

The experimental setup has been described in more detail in [3], hence we dwell on it only briefly. NaK molecules have been formed in thermal cells made from special alkali-metal-resistant glass and attached to a vacuum system via a dry valve. Characteristic working temperatures of the metal containing reservoir (weight ratio Na:K$\approx$1:3) were $T\approx 525-575$ K. A number of visible blue-green Spectra Physics 171 Ar^+-laser lines (see Table I) have been used to excite $D\ ^1\Pi v(J)\leftarrow X\ ^1\Sigma^+ v''(J'')$ transitions. Visible LIF lines, originating from the $\sim$1 mm diam laser excitation region, have been viewed at right angles to the exciting laser beam, imaged onto the entrance slit of a double-monochromator and resolved by a 1200 lines/mm grating blazed in the first order, providing an overall spectral resolution of $\sim$0.03 nm. Polarizers were used to realize all possible linear polarization options in rectangular excitation-observation geometry. $D\ ^1\Pi v(J)$ state selection has been maintained by finding in the overall LIF spectrum the particular LIF progressions mentioned in [12] and originating from the chosen $v(J)$ level under study. The signal from a photomultiplier was recorded using the photon counting technique.

The electric field, either dc or RF, was applied to the carefully polished stainless steel Stark plates, $\sim$0.8 cm in diameter, separated by a 1.2 mm gap. The RF field 5–900 MHz, usually possessing an amplitude of $\sim$5 V, required to induce resonant Λ-doublet mixing, was produced either by a

TABLE I. Exciting laser wavelengths (λ_{exc}), experimentally obtained values of electric RF-ODR resonance frequencies (f_0), Λ-doubling factors (q), and PEDM values (d) for NaK ($D\ ^1\Pi$) v,J states.

λ_{exc} (nm)	v	J	f_0 (MHz)	q (10^{-5} cm^{-1})	d (D)
496.5	1	27	346±2	1.526±0.006	5.9±0.2
501.7	3	23	242±3	1.461±0.010	6.4±0.2
496.5	3	43	853±3	1.503±0.004	
496.5	4	19	172±2	1.509±0.010	6.6±0.2
496.5	7	8	30±2	(1.389±0.070)[a]	
				(1.437±0.070)[b]	
488.0	7	20	172±2	(1.365±0.010)[a]	6.2±0.3
				(1.416±0.010)[b]	
488.0	7	23	249±2	1.504±0.008	6.4±0.2
496.5	11	46	673±3	1.038±0.003	5.1±0.2
476.5	12	7	17±1.5	1.012±0.080	4.7±0.6
476.5	14	19	162±3	1.421±0.020	5.9±0.3
488.0	22	35	448±2	1.185±0.004	4.6±0.2

[a]For isotope ^{23}Na ^{41}K.

[b]Values transformed from ^{23}Na ^{41}K to ^{23}Na ^{39}K.

Wavetek RF generator (1–300 MHz), or by Mini-circuit voltage controlled oscillators (20–900 MHz), followed by a high power amplifier (Mini-circuit ZHL-2-12). The RF field frequency f was swept repeatedly, with a 1–2 MHz step within the expected double resonance region by means of a computer-driven dc power supply. The typical signal storage time was 20–90 min, with overall averaging during 20–60 s for each RF value.

It was noticed that specific features could arise, under particular conditions, in the resonance region, leading in some cases to the trend to exhibit some parasitic peaks in the resonance signal. At the beginning, we were inclined to ascribe these peaks to the influence of some hyperfine structure (HFS). Careful testing convinced us, however, that these peaks were artifacts since their position and shape have been fully determined by a particular arrangement of the RF loop. The parasitic peaks disappeared after carefully matching the connecting line parameters.

C. Signal processing

Typical examples of the experimentally observed $\mathcal{E}$ dependence of the intensity ratio I_f/I_p are given in Fig. 2. The fitting (see the solid curve in Fig. 2) has been performed using an approach that involves diagonalization of the Hamiltonian, accounting for dc Stark mixing between all $J \pm \Delta J$ levels with $\Delta J \leqslant 2$ in the initial, excited, and final rovibronic states of a LIF transition, see Ref. [3] for details. As tested in [3], the fitting yields, with satisfying accuracy, the desired Δ_{ef}/d value, provided that the upper level relaxation rate Γ is known at least within ~30% accuracy. At first we used Γ values based on the NaK $D\ ^1\Pi\ v(J)=7(23)$ lifetime measured in [23] as $\tau=\Gamma^{-1}=20$ ns. However, it appeared also possible to obtain Γ directly from the RF-ODR signal contour (see Fig. 3), yielding lifetimes within 13–23 ns for various $v(J)$ levels under study [24]. The approach [3] implies broad line excitation under conditions when ground-state optical pumping effects [25] can be neglected. To check the possible influence of the above effects, the $\mathcal{E}$ dependencies of I_f/I_p ratios have been recorded at various exciting laser regimes; see Fig. 2. We have also checked that the dependences obtained at different excitation-observation geometries and polarizations of the exciting light ($\mathbf{E}$) and fluorescence light ($\mathbf{E_f}$) vectors yielded the same Δ_{ef}/d ratio.

Some of the experimental RF-ODR signals obtained are presented in Fig. 3. Resonance frequencies f_0 (see Table I) have been obtained from Lorentz shape contour fitting. It was proved experimentally that the f_0 values remain the same at different RF electric field amplitudes.

D. Hyperfine structure

Let us now consider the possible influence on the $\mathcal{E}$ dependencies of I_f/I_p and on the RF-ODR signals of the hyperfine (HF) interaction in the NaK $D\ ^1\Pi$ state. We will first focus on RF-ODR signals. It is clear that, owing to the $\Delta F=0$ selection rule [26], one has to examine the difference in the HFS patterns of e and f components. The origin of different HF splitting is related to the geometrical properties of the WF, since the WF with $\epsilon=1$ ($\epsilon=-1$) in Eq. (2) is symmetric (antisymmetric) with respect to reflection in the plane of molecular rotation, the respective molecular orbitals lying in the rotational plane and at right angles to it [27]. From the well known expression for the magnetic HFS interaction operator $\langle {}^1\Pi_{e/f}|\hat{\mathbf{H}}_{\mathbf{mg}}|{}^1\Pi_{e/f}\rangle$ [26], the magnetic HF energy terms are the same for the e and f components, being dependent on Λ^2, thus having no influence on the RF resonance signal. Nevertheless, in the next approximation one has to account for the existence of the nonzero magnetic HFS operator matrix element $\langle {}^1\Sigma^+|\hat{\mathbf{H}}_{\mathbf{mg}}|{}^1\Pi_e\rangle$, which leads to a HF shift of the e component only, $\Delta E_e^{mg}=c_I\mathbf{IJ}$ [26]. The estimated c_I value is proportional to the ratio of the $^1\Pi$ state q factor and the rotational constant B_v, namely $c_I=aq_v/B_v$, a being the magnetic HFS constant

$$a=\frac{2\mu_0\mu}{I}\,\overline{r^{-3}}, \tag{3}$$

where μ is the nuclear magnetic moment, μ_0 is the Bohr magneton, and the averaging includes only the electrons giving nonzero contribution to the electronic orbital momentum $\mathbf{L}$.

Electric quadrupole HF interaction may also cause a different energy shift for e,f levels. The respective Hamiltonian $\hat{\mathbf{H}}_{\mathbf{Q}}$ can be written, in standard multipole form, as $\hat{\mathbf{H}}_{\mathbf{Q}}=\Sigma_{q=-2}^{2}(-1)^q V_q^{(2)}Q_{-q}^{(2)}$. Here the nuclear quadrupole moment Q operator $Q_q^{(2)}$ acts on the nuclear coordinates only while the electric field gradient operator $V_q^{(2)}$ acts upon the electron coordinates. The electric quadrupole interaction constant $b_{\Lambda\Lambda'}$ can be written as [28]

$$\begin{aligned} b_{\Lambda\Lambda'}&=eQq_{\Lambda\Lambda'}\\ &=2eQN(-1)^{\mu}\langle -\Lambda-\mu\|eC_{-\mu}^{(2)}(\delta,\phi)\overline{r^{-3}}\|-\Lambda\rangle, \end{aligned} \tag{4}$$

where $C_{-\mu}^{(2)}(\delta,\phi)$ is proportional to a spherical function [29], N denotes the number of electrons, and the $\overline{r^{-3}}$ value is averaged over all electrons. As already pointed out in [26], the matrix elements in Eq. (4) with $\Delta\Lambda=\pm 2$ can differ from zero; see also [30]. To consider the contribution of these matrix elements to the $^1\Pi$ state HFS, one has to apply the respective quadrupole interaction operator H_Q, which is a second rank tensor, to our WF given by Eq. (2), thus arriving at the energy shift of the e,f components:

$$\Delta E_{e/f}^{Q}\equiv\Delta E_{\pm}^{Q}=eQq_{11}X_1\pm eQq_{1\text{-}1}X_2, \tag{5}$$

where X_1 and X_2 depend only on J, I, and F. Here the diagonal (longitudinal) matrix element $b_{11}=eQq_{11}$ gives the usual HF energy for symmetric top molecules [26,31], in which K plays the same role as Λ for the diatomics, while the nonzero off-diagonal (transversal) matrix elements $b_{1\text{-}1}=eQq_{1\text{-}1}$ are responsible for different HF energies in e and f Λ-doubling components, which is specific for the $^1\Pi$ state.

It is not an easy matter to estimate the magnetic HFS constant a and field gradient values $q_{\Lambda\Lambda'}$ since these quantities include the value of $\overline{r^{-3}}$ averaged over the electrons; see Eqs. (3) and (4). For this purpose a preliminary attempt has been made to perform *ab initio* calculations [8] by the internally contracted CI method [9]. The estimated values are (in MHz) $a^{\mathrm{Na}}=4.1$, $a^{\mathrm{K}}=0.08$, $b_{11}^{\mathrm{Na}}=0.1$, $b_{11}^{\mathrm{K}}=-0.8$,

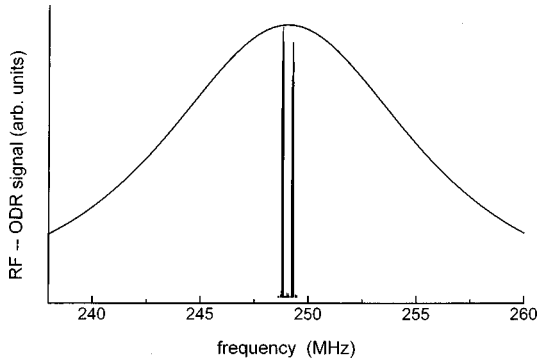

FIG. 4. Expected HF components position of RF-ODR signal for $D\ ^1\Pi\ J=23$.

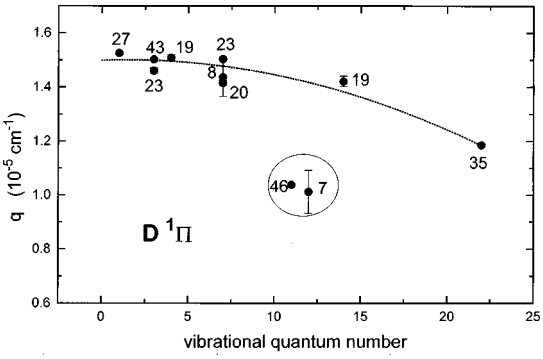

FIG. 5. NaK $D\ ^1\Pi$ state $q(v)$ values for various J obtained from RF-ODR measurements.

$b_{1\text{-}1}^{\mathrm{Na}}=-0.8$, and $b_{1\text{-}1}^{\mathrm{K}}=-0.06$. The calculated positions of HF e-f transitions are presented in Fig. 4. Similar and somewhatsmaller HFS parameters have been obtained using the GAMESS program package [32]. It should be noted that all HFS parameters were estimated without accounting for local spin-orbit $D\ ^1\Pi\sim d\ ^3\Pi$ perturbations. As can be seen from the figure, the scale of HF splitting is ~0.5 MHz, the RF-ODR signal width being typically ~15–25 MHz; see Fig. 3. This allows us to suggest that the HFS influence on the position of the resonance signal, and, hence, on q values is negligible. The same data about HFS coefficients have been used to check the possible HFS influence on the $\mathcal{E}$ dependencies of intensity ratios I_f/I_p. The respective HFS energy levels and transition matrix elements have been calculated by H-matrix diagonalization in an external dc electric field. Calculation was performed for the $v(J)=12(7)$ state, with the smallest J, because of the greatest expected HFS influence. The results obtained, using Γ, q, and d values from Ref. [3], showed that relative changes in $\mathcal{E}$ dependencies of $I_Q/I_{P,R}$ did not exceed 3% for the smallest $\mathcal{E}=10$ V/cm value used in our experiments, falling asymptotically to zero with increasing $\mathcal{E}$. The above simulations permitted us to conclude that, if our HFS constants are not too underestimated, the inaccuracy in experimentally obtained q and Δ_{ef}/d values due to HFS influence is negligible.

III. RESULTS

The resonance frequencies f_0 for various $v(J)$ levels, averaged over the series of measurements, are presented in Table I. These values allowed us to determine the NaK $D\ ^1\Pi$ state q factor values defined by Eq. (1); see Table I. The errors given in the table reflect the divergence of the results in various experiments. The two levels, namely 7(8) and 7(20), belong to the ^{23}Na ^{41}K isotope molecule [12], and their q values have been transformed into the ones expected for ^{23}Na ^{39}K as $q^{39}\approx q^{41}(\mu^{41}/\mu^{39})^2$, where μ^{41} and μ^{39} are the respective reduced molecular masses. Since the J values are not too large, we have depicted, in Fig. 5, the q values from Table I as dependent on v, and approximated them by a parabolic function (dashed line). As is clear at first glance, all q values, except for the ones for 11(46) and 12(7), do not contradict too much the quadratic $q(v)$ dependence, when the J dependence is ignored. The q values for 11(46) and 12(7) drop out completely from the general picture, which inclines one to think of local perturbations caused by the $D\ ^1\Pi\sim d\ ^3\Pi$ spin-orbit interaction; see Sec. VII.

The experimental q values from Table I, together with Δ_{ef}/d ratios obtained as a single fitting parameter from I_f/I_p $\mathcal{E}$ dependencies, permitted us to pass to electric dipole moments d, which are also listed in Table I. In two cases, namely for the 3(43) and 7(8) states, we found it impossible to get reliable Δ_{ef}/d ratios, and, thus, d values are not presented for these states. The d value errors in Table I reflect mainly the variations of Δ_{ef}/d in different experiments, as well as the inaccuracy in measuring the gap between the Stark plates. $D\ ^1\Pi$ state d values are depicted in Fig. 6 as dependent on v. Again, d values for perturbed 11(46) and 12(7) levels fall out markedly from the $d(v)$ dependence.

IV. Λ-DOUBLING CONSTANTS

A. $q(v,J)$ fitting

The $q(v,J)$ values measured in the present work, see Table I, have been processed together with the $q(v,J)$ data, which have been extracted by us from the traditional high resolution spectroscopy data given in [12]. The latter have been obtained from the differences between experimental rovibrational term values for PR and Q branches originating from the same rotational state J. Since the absolute accuracy of term value measurements in [12] was not better than 0.05 cm^{-1}, the only way to evaluate q values was averaging over a group of closely situated J levels with sufficiently high $J>60$. The results are presented in Table II. The overall experimental $q(v,J)$ set from Table II was treated by the

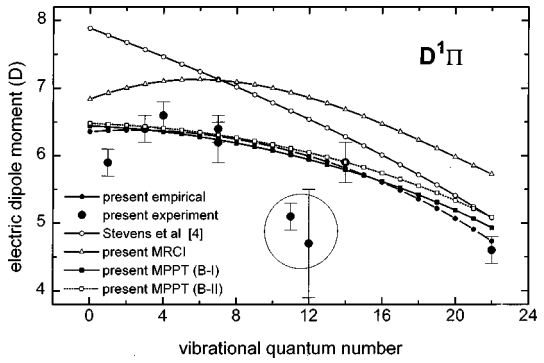

FIG. 6. $D\ ^1\Pi$ state $d(v)$ values.

TABLE II. Λ-doubling constants (in 10^{-5} cm^{-1}): q^{exper}, measured in the present work or obtained by processing Ref. [12] data; q^{fit}, obtained by fitting according to Eq. (6); and q^{se}, obtained by semiempirical estimation with $L^{el}=1.87$. The fitting parameters q_i (cm^{-1}), see Eq. (6), are $q_e=1.570(-05)$, $q_{v1}=-5.15(-08)$, $q_{v2}=-4.665(-09)$, and $q_J=-3.069(-10)$.

$v(J)$	q^{exper}	q^{fit}	q^{se}
	Present data		
1(27)	1.526(6)	1.538	1.427
3(23)	1.461(10)	1.528	1.432
3(43)	1.503(4)	1.487	1.396
4(19)	1.509(10)	1.524	1.419
7(8)	1.437(70)	1.501	1.419
7(20)	1.416(10)	1.490	1.420
7(23)	1.504(8)	1.486	1.420
11(46)	1.038(3)	1.379	1.326
12(7)	1.012(80)	1.427	1.380
14(19)	1.421(20)	1.381	1.341
22(35)	1.185(4)	1.174	1.154
	Data based on Ref. [12]		
1(66)	1.51(20)	1.425	1.365
1(95)	1.20(13)	1.281	1.255
5(105)	0.98(11)	1.184	1.209
6(75)	1.39(35)	1.340	1.302
10(101)	1.15(22)	1.145	1.170
17(93)	1.15(20)	1.063	1.068

weighted least-squares method (LSM) in the framework of the following Dunham-like model:

$$q(v,J)=q_e+q_{v1}(v+1/2)+q_{v2}(v+1/2)^2+q_JJ(J+1). \tag{6}$$

The fitted $q(v,J)$ values for $D\ ^1\Pi$ v,J states under study are presented in Table II, along with fitting parameters q_i entering Eq. (6). As may be seen, q is diminishing, as v and J are increasing. It is worth mentioning that the authors of Ref. [12] have presented the only parameter $q_0=1.16\pm0.07\times10^{-5}$ cm^{-1} obtained from simultaneous fitting of all rovibrational levels of both $D\ ^1\Pi$ and $X\ ^1\Sigma^+$ electronic states, since the accuracy of their measurements was not sufficient for determining the v,J dependence of q values. At first glance, the q_0 value given in [12] may seem smaller than the respective value in the present work, since $q_e=1.57\times10^{-5}$ cm^{-1}. If, however, one takes into account that q_0 in [12] is related to J from 60 to 106, and v from 1 to 22, it is easy to arrive from Eq. (6) at $q(\bar{v}=11,\bar{J}=83)=1.24\times10^{-5}$ cm^{-1}, which is much closer to the q_0 value given in Ref. [12].

B. Semiempirical interpretation

$D\ ^1\Pi$ *state*

In order to clarify the reason for a decline in q values with v and J, we have performed $q(v,J)$ calculations within a wide v and J range, namely $0<v<25$ and $1<J<100$, based on the $D\ ^1\Pi\sim C\ ^1\Sigma^+$ interaction:

$$q_\Pi(v,J)=2\sum_{v_\Sigma}\frac{\langle v_\Pi^J|L^{el}(R)/(2\mu R^2)|v_\Sigma^J\rangle^2}{E^\Pi_{u_\Pi J}-E^\Sigma_{v_\Sigma J}}\approx|L^{el}|^2S(v,J), \tag{7}$$

where

$$S(v,J)=2\sum_{v_\Sigma}\frac{|\langle v_\Pi^J|1/2\mu R^2|v_\Sigma^J\rangle|^2}{E^\Pi_{v_\Pi J}-E^\Sigma_{v_\Sigma J}},\quad L^{el}(R)=L^{el}=\text{const}, \tag{8}$$

and the vibrational WF's $|v^J\rangle=\chi_{vJ}(R)$ are eigenfunctions of the radial Schrödinger equation:

$$\left[-\frac{1}{2\mu}\frac{d^2}{dr^2}+U_J(R)\right]\chi_{vJ}(R)=E_{vJ}\chi_{vJ}(R). \tag{9}$$

Here μ is the reduced molecular mass, $U_J(R)=U(R)+[J(J+1)-\Lambda^2]/(2\mu R^2)$ is the effective (centrifugally distorted) internuclear potential function, and $U(R)$ is the rotationless potential based on the Born-Oppenheimer (BO) separation. In the present work we used for the NaK $D\ ^1\Pi$ state the BO potential calculated in Ref. [12] with high accuracy by the inverted perturbation approach (IPA) [33,34], while for the $C\ ^1\Sigma^+$ state the Rydberg-Klein-Rees (RKR) potential has been constructed using Dunham molecular constants from Ref. [35]. To solve numerically the Schrödinger equation (9), we implemented the iterative renormalized Numerov algorithm [36], combined with the Richardson extrapolation [37]. An efficient phase-matching method [38] was employed to find the eigenvalues. This construction allowed us to reduce the relative errors in $S(v,J)$ values to 10^{-5}–10^{-6}.

It turned out that the $S(v,J)$ values calculated according to Eq. (8) exhibit a monotonous decrease with increasing v and J. Further, using the $S(v,J)$ values thus obtained we transformed experimental $q(v,J)$ values into electronic L-uncoupling matrix elements $L^{el}\approx\sqrt{q_{exp}(v,J)/S(v,J)}$. The L^{el} values thus obtained appeared to be equal to 1.87, the spread not exceeding 10%. This shows that, first, the decrease of $q(v,J)$ with an increase in v and J is determined mainly by the increase with R in potential difference $U_{D\ ^1\Pi}(R)-U_{C\ ^1\Sigma^+}(R)$ and, second, that the $L^{el}=$const assumption holds with quite a good approximation, which is perfectly understandable, since, as can be seen from Eq. (7), the R dependence of $q(v,J)$ within the narrow R range is mainly determined by the $1/R^2$ factor. The semiempirical values q^{se} calculated according to Eqs. (7) and (8) with $L^{el}=1.87$ are presented in Table II. It is interesting that the electronic matrix element of electron-rotation interaction exceeds considerably the value $l(l+1)=\sqrt{2}$. This can be expected from a pure precession approximation [10,39] under the simplest single configuration model for the perturbed $D\ ^1\Pi(\sigma 4s_K,\pi 3p_{Na})$ and the perturbing $C\ ^1\Sigma^+(\sigma 4s_K,\sigma 3p_{Na})$ electronic states. This fact can probably be explained by a considerable admixture of corresponding πd and σd atomic electronic configurations in molecular electronic WF's. Indeed, assuming, for the sake of simplicity, the equal contribution of πd and σd configurations to the respective $D\ ^1\Pi$ and $C\ ^1\Sigma^+$ states, that is, $|\pi(D\ ^1\Pi)\rangle\approx C_1|\pi p\rangle+C_2|\pi d\rangle$ and $|\sigma(C\ ^1\Sigma^+)\rangle\approx C_1|\sigma p\rangle+C_2|\sigma d\rangle$, where $C_1^2+C_2^2=1$, one easily arrives at

$$\langle D\ ^1\Pi|\hat{\mathbf{L}}|C\ ^1\Sigma^+\rangle \approx C_1^2\sqrt{2}+C_2^2\sqrt{6}\approx\sqrt{2}+C_2^2(\sqrt{6}-\sqrt{2})$$
$$\approx 1.87, \tag{10}$$

which allows us to conclude that the contribution of the πd and σd configurations is ~44% each. Of course, it is a very gross approximation to assume the same $p\sim d$ mixing for σ and π orbitals. The difference, however, is not too large ($\leqslant$20%) at small internuclear distance where the L-uncoupling matrix elements are most important.

Indeed, the population analysis of multireference configuration-interaction (MRCI) wave functions, see Sec. VI for details, has shown that the πd configuration contributes to the $D\ ^1\Pi$ state from ~25% at $R=8$ a.u., up to ~40% at $R=5$ a.u., and to the $C\ ^1\Sigma^+$ state from ~20% up to ~35%, respectively. Similar estimates performed for the lower $A\ ^1\Sigma^+$ and the higher (4) $E\ ^1\Sigma^+$ states revealed negligible σd contribution as compared to the one in the $C\ ^1\Sigma^+$ state for the same R region. Besides, the $S(v,J)$ factors in Eq. (8) calculated for $A\ ^1\Sigma^+$ and (4) $E\ ^1\Sigma^+$ states revealed to be 2–3 times smaller than the respective factors for the $C\ ^1\Sigma^+$ state, due to energy considerations. It is obvious that the $S(v,J)$ factors for (4) $E\ ^1\Sigma^+$ and $A\ ^1\Sigma^+$ states possess different signs, which practically compensate their contributions to the $D\ ^1\Pi$ state Λ-doubling constants.

We may thus formulate the following conclusions regarding the behavior of q values for the NaK $D\ ^1\Pi$ state: (i) the unique perturber $D\ ^1\Pi\sim C\ ^1\Sigma^+$ approximation [10] is quite valid for the $D\ ^1\Pi$ state Λ doubling due to the fact that the contributions of upper (4) $E\ ^1\Sigma^+$ and lower $A\ ^1\Sigma^+$ states are, first, small with respect to the $C\ ^1\Sigma^+$ contribution and, second, practically compensate each other; (ii) the fact that the pure precession approximation [39] (with $l=1$ for a single πp configuration) does not hold, along with relatively large q values, stems from the considerable contribution of πd configurations to the electronic WF's of interacting $D\ ^1\Pi\sim C\ ^1\Sigma^+$ states at small R; (iii) a decrease of q values with increasing v and J has nothing to do with the decrease in the L-uncoupling matrix element, but is mainly connected with the increase with R in the difference potential between $D\ ^1\Pi$ and $C\ ^1\Sigma^+$ states.

$B\ ^1\Pi$ *state*

Let us now estimate, by means of Eq. (7), contributions of the $A\ ^1\Sigma^+$ and $C\ ^1\Sigma^+$ states to the q_{vJ} values of the NaK $B\ ^1\Pi$ state. It is interesting to mention that the unique perturber approximation breaks down in this case [2,15] since the lower-lying $A\ ^1\Sigma^+$ state and the higher-lying $C\ ^1\Sigma^+$ state produce comparable contributions, with opposite signs, to the $B\ ^1\Pi$ state q values. This leads to a noticeable decrease in q values, which are smaller by almost an order of magnitude than those of the $D\ ^1\Pi$ state. Unlike the $D\ ^1\Pi$ and $C\ ^1\Sigma^+$ states, the single configuration approximation is valid for the interacting $B\ ^1\Pi(\sigma 3s_{\mathrm{Na}},\pi 4p_{\mathrm{K}})$ and $A\ ^1\Sigma^+(\sigma 3s_{\mathrm{Na}},\sigma 4p_{\mathrm{K}})$ states; we thus get $\langle B\ ^1\Pi|\hat{\mathbf{L}}|A\ ^1\Sigma^+\rangle=\sqrt{2}$. In order to estimate $\langle B\ ^1\Pi|\hat{\mathbf{L}}|C\ ^1\Sigma^+\rangle$, let us recall that the $C\ ^1\Sigma^+$ state is built up by the σp molecular orbital only to the extent of 56%, which, in the simplest case, can be assumed as a primitive linear combination of atomic orbitals (LCAO), $|\sigma p\rangle=2^{-1/2}[|\sigma 3p_{\mathrm{Na}}\rangle+|\sigma 4p_{\mathrm{K}}\rangle]$, yielding

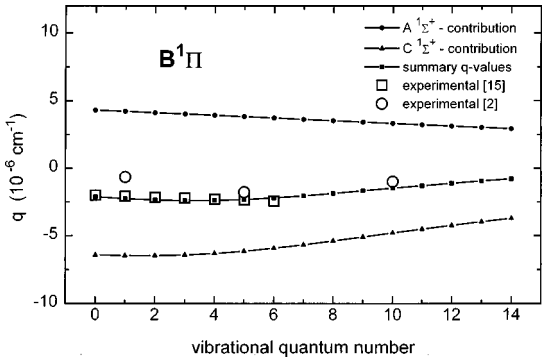

FIG. 7. $B\ ^1\Pi$ state q factors.

$\langle B\ ^1\Pi|\hat{\mathbf{L}}|C\ ^1\Sigma^+\rangle\approx 0.75$. The $S(v,J)$ factors, see Eq. (8), were calculated using RKR potentials. The resulting $A\ ^1\Sigma^+$ and $C\ ^1\Sigma^+$ contributions to the $B\ ^1\Pi$ state q factors thus calculated are presented in Fig. 7. The total $q(v,J)$, as may be seen from the figure, are in satisfactory agreement (within 10%) with the high accuracy experimental data from Ref. [15] obtained by Doppler-free laser polarization spectroscopy. The discrepancy with q values measured indirectly in [2] by the dc Stark effect can be, most likely, connected with the drawbacks of the experimental method applied. In particular, the Λ-doubling constants presented in Ref. [2] for $v=1$, 5, and 10 were obtained from the $\mathcal{E}$ dependencies of the ratio of forbidden to allowed intensities for a number of J levels varying from $J=4$ up to $J=24$ for each v. For these levels Δ_{ef} is smaller than the natural linewidth and, hence, the $e\sim f$ Stark mixing measurements may not be sensitive enough to the value of q factor.

Since the molecular $\hat{\mathbf{L}}_{\pm}^{\mathrm{mol}}$ operator is defined with respect to the center of mass of the molecule, while the exploited atomic orbitals are centered at the nucleus of the respective atom, the present estimates of the $L_{\pm}$ matrix elements should be, in general, corrected in accordance with the coordinate origin shift effect pointed out by Colbourn and Wayne [40]. The molecular $\hat{\mathbf{L}}_{\pm}^{\mathrm{mol}}$ operator is connected with its atomic counterpart as

$$\hat{\mathbf{L}}_{\pm}^{\mathrm{mol}}=\hat{\mathbf{L}}_{\pm}^{A}-\frac{m_B R}{m_A+m_B}\,\hat{\mathbf{P}}_{\pm}, \tag{11}$$

where $\hat{\mathbf{L}}_{\pm}^{A}$ is the angular momentum operator with respect to the nucleus A, $\hat{\mathbf{P}}$ is the momentum of the electrons, and m_A and m_B are the atomic masses. From the well-known commutation relation $\hat{\mathbf{P}}=\mathrm{i}(\mathrm{m}_e/\hbar)[\hat{\mathbf{H}}^{\mathrm{el}},\hat{\mathbf{d}}]$, where m_e is the electron mass, $\hat{\mathbf{H}}^{\mathrm{el}}$ is the electronic Hamiltonian, and $\hat{\mathbf{d}}$ is the electric dipole moment operator, one gets from Eq. (11)

$$\langle n|\hat{\mathbf{L}}_{\pm}^{\mathrm{mol}}-\hat{\mathbf{L}}_{\pm}^{A}|m\rangle=\frac{m_e m_B R}{\hbar(m_A+m_B)}\,(E_n^{\mathrm{el}}-E_m^{\mathrm{el}})\langle n|\hat{\mathbf{d}}_{\pm}|m\rangle, \tag{12}$$

where $E_n^{\mathrm{el}}-E_m^{\mathrm{el}}=\Delta U(R)$ is the difference potential and $\langle n|\hat{\mathbf{d}}_{\pm}|m\rangle$ is the matrix element of the transition dipole moment. The application of Eq. (12) to the matrix elements $L_{\pm}$ between the states under consideration shows that, within the internuclear distance between 4 and 10 a.u., the maximum corrections for $\langle D\ ^1\Pi|\hat{\mathbf{L}}_{\pm}|C\ ^1\Sigma\rangle$, $\langle B\ ^1\Pi|\hat{\mathbf{L}}_{\pm}|C\ ^1\Sigma\rangle$, and

$\langle B\ ^1\Pi|\hat{\mathbf{L}}_{\pm}|A\ ^1\Sigma\rangle$ matrix elements are 0.3%, 2.1%, and 15.5%, respectively. The correction values were calculated using the RKR potential curves of the interacting states and the corresponding *ab initio* transition dipole moment functions given in Ref. [41]. It is worth mentioning that the above corrections for the states under consideration appeared to be rather small as compared to those of the ground states owing to the fact that these states have a significant Rydberg character at relatively small internuclear distances.

V. INVERSION PROCEDURE FOR DIPOLE MOMENT FUNCTION

The PEDM $d(v,J)$ for a particular vibrational-rotational level means the expectation value of the PEDM R function $d(R)$, namely $d(v,J)=\langle v^J|d(R)|v^J\rangle$, where $d(R)$ is, in its turn, the electric dipole moment operator expectation value over the respective electronic state WF's. In order to deduce $d(R)$ from the experimentally measured $d(v,J)$, the realistic functional $d(R)$ form is of critical importance. Most conveniently, $d(R)$ can be represented as a linear superposition of some basis functions $f_i(R)$: $d(R)=\Sigma_i a_i f_i(R)$, where the coefficients a_i are given by a system of linear equations:

$$d(v,J)=\sum_{i=0}^{N} a_i\langle v^J|f_i(R)|v^J\rangle, \tag{13}$$

which is generally overdetermined and can be solved by the standard LSM [42] routine. Usually the simplest R-function forms such as R^i, $(R-R_e)^i$ or $(R/R_e-1)^i$ are used as basis functions $f_i(R)$, R_e being the equilibrium internuclear distance for a particular electronic state. Employment of these functions leads, however, to an unphysical asymptotic behavior of $d(R)$, both at small $(R\rightarrow 0)$ and large $(R\rightarrow\infty)$ internuclear distances, often accompanied by noticeable $d(R)$ oscillations that increase with the power i. Besides, such a functional form leads to an increase in linear dependence in the equation system (13), in particular when the number of basis functions is growing, thus producing solution instability, which, in its turn, produces large errors in the determination of coefficients a_i. To overcome these difficulties we used the functional form, which has been successfully exploited before in the IPA method [34] only, namely

$$f_i(R)=P_i(x)\exp(-x^{2n}), \tag{14}$$

where $P_i(x)$ are Legendre polynomials of order i, x is a smooth function of R, while n is typically 2 or 3. It is obvious that the Gaussian part of Eq. (14) provides a smooth cutoff, avoiding any unphysical oscillations of the moment, while Legendre polynomials form an orthogonal basis set that leads to fast convergence of expansion (14) and helps to minimize the linear dependence in Eq. (13).

For the R dependence of x we used, following Ref. [34], the nonlinear interpolation $x=(R-R_e)(R_{\max}-R_{\min})/[(R_{\min}+R_{\max})(R_e+R)-2R_{\min}R_{\max}-2RR_e]$, where $R_{\max}$ and $R_{\min}$ were chosen as the outermost and innermost classical turning points of the internuclear potential, which correspond to the highest vibrational level to be fitted. For the $D\ ^1\Pi$ state it is the level $v=22$, thus $R_{\max}=5.97$ Å and $R_{\min}=3.31$ Å, while for the $B\ ^1\Pi$ state it is the level $v=14$, thus $R_{\max}=5.85$ Å and $R_{\min}=3.37$ Å. Such an interpolation procedure treats the inner and outer turning points with comparable weights and reduces markedly the number of necessary Legendre polynomials in Eq. (14). The $d(R)$ functions for the $D\ ^1\Pi$ and $B\ ^1\Pi$ states were approximated by Eq. (14) with the number N of the basis functions varying from 3 to 5, depending on the model. The a_i parameters were determined, using the weighted LSM with singular value decomposition of the plan matrix to control the linear dependence of normal equations arisen in LSM [42].

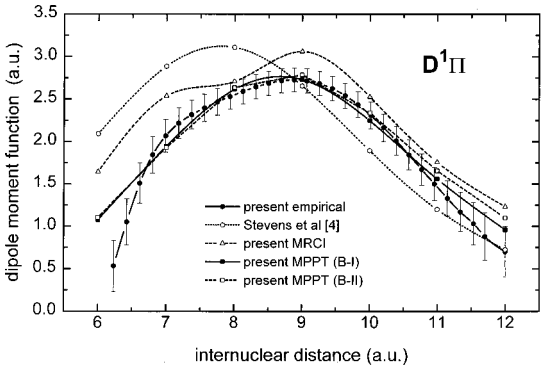

FIG. 8. $D\ ^1\Pi$ state $d(R)$ functions.

For the NaK $D\ ^1\Pi$ state the experimental $d(v,J)$ values obtained in the present work (Table I, Fig. 6) have been used as the basis data. In doing so, we have excluded d values for the perturbed $v(J)$ levels 11(46) and 12(7), see Sec. VII for details. The resulting empirical function $d(R)$ is reproduced in Fig. 8 (solid circles). To prove the adequacy of the dependence thus obtained, we have exploited it to solve a direct problem, that is, to calculate $D\ ^1\Pi$ state d values at $J=1$ for v ranging from 0 to 22 (small solid circles in Fig. 6).

To demonstrate the viability of the method suggested, we have determined the empirical dipole moment function $d(R)$ also for the $B\ ^1\Pi$ state of NaK using $d(v,J)$ measurements for four levels $v=1$, 5, 10, and 14, carried out in Ref. [2] (see the solid circles in Fig. 9). The resulting $d(R)$ function is presented in Fig. 10 (small solid circles), while the corresponding PEDM's $d(v)$ are presented in Fig. 9 (small solid circles). It has to be mentioned that the determination of the $B\ ^1\Pi$ state $d(v)$ for $v=1$, 5, and 10 from the measured q/d ratios in Ref. [2] has been based upon q_v evaluations that, for $v=1$ and 5, appeared to be considerably smaller than the q_v values obtained later by the authors of Ref. [15] from Doppler-free polarization spectroscopy measurements. If we

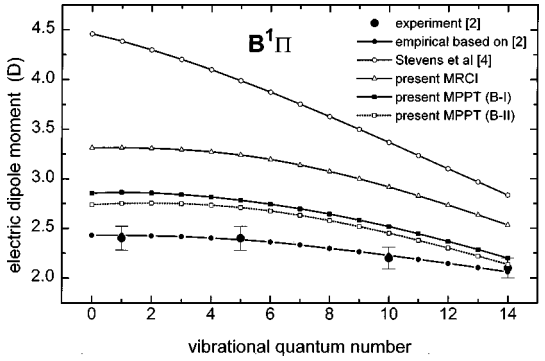

FIG. 9. $B\ ^1\Pi$ state $d(v)$ functions.

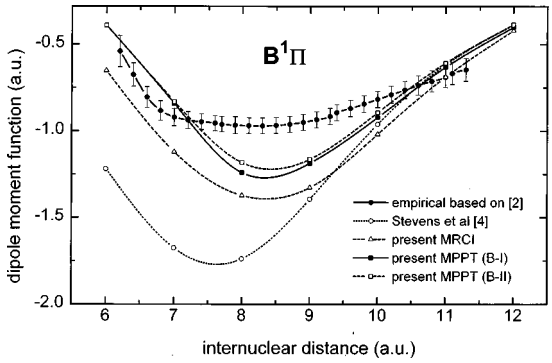

FIG. 10. $B\ ^1\Pi$ state $d(R)$ functions.

believe that the q/d ratios measured in Ref. [2] from the dc Stark effect induced forbidden/allowed LIF line intensity ratios are correct, it is not excluded that the respective dipole moment values are larger than the ones presented in Ref. [2]. For instance, if one takes $q_{v=5}=2.36\times10^{-6}$ cm^{-1} [15] instead of $q_{v=5}=1.77\times10^{-6}$ cm^{-1} [2], the d value with $v=5$ becomes 3.2 D instead of 2.4 D.

VI. *AB INITIO* DIPOLE MOMENT CALCULATIONS

We have performed two independent series of *ab initio* all-electron calculations of the dipole moment functions using substantially different approximations for electronic eigenstates and different approaches to dipole moment evaluation.

A. Expectation-value MRCI calculations

In the first series the dipole moments for the $D\ ^1\Pi$ and $B\ ^1\Pi$ states were computed as expectation values of the electric dipole operator with conventional multireference configuration interaction (MRCI) WF's. The atomic basis sets $(17s12p7d1f)/[12s9p5d1f]$Na and $(17s13p7d1f)/[11s9p5d1f]$K used in the MRCI calculations were taken from Ref. [43] and Ref. [44], respectively. Molecular orbitals (MO's) were obtained from restricted Hartree-Fock (RHF) calculations on the ground state of the NaK^{2+} ion. Eight MO's corresponding to $1s2s$(Na) and $1s2s2p3s$(K) cores were frozen after the RHF step and 14 electrons including the $2p$(Na) and $3p$(K) core were correlated. The reference space was spanned by all possible arrangements of two valence electrons among five σ and four π active MO's. The CI space has included all the reference space configurations plus all configurations generated by single and double excitations of the reference functions. The dimension of the MRCI problem was about 3×10^5. All calculations mentioned above were performed using the GAMESS program package [32]. The resulting MRCI $d(R)$ functions are presented in Fig. 8 for the $D\ ^1\Pi$ state and in Fig. 10 for the $B\ ^1\Pi$ state. The respective MRCI $d(v)=\langle v|d(R)|v\rangle$ values are presented in Fig. 6 for $D\ ^1\Pi$ $v=0$–22 and in Fig. 9 for $B\ ^1\Pi$ $v=0-14$ states.

B. Finite-field MPPT calculations

The finite-field method derives the PEDM estimates from the variation of electronic state energy E under a perturbation by a small finite electric field $\mathcal{E}$ [45–47]:

$$d=-\left.\frac{dE(\mathcal{E})}{d\mathcal{E}}\right|_{\mathcal{E}=0}\approx\frac{E(-\Delta\mathcal{E}/2)-E(\Delta\mathcal{E}/2)}{\Delta\mathcal{E}},\qquad(15)$$

where $\Delta\mathcal{E}$ is the step size of the finite-difference scheme. The diagonal Hellmann-Feynman theorem ensures equivalence between the derivatives in Eq. (15) and the corresponding expectation value of the electric dipole operator for the exact electronic WF. For approximate solutions of the electronic problem appearing in practical *ab initio* calculations such equivalence usually does not hold, and the finite-field estimates are, as a rule, believed to be less sensitive to the quality of approximation [46].

The necessary $E(\mathcal{E})$ values were calculated by the state-selective multipartitioning perturbation theory (MPPT) [48], using the recently developed program [49] interfaced to the MOLCAS suite of electronic structure codes [50]. Two differently constructed Gaussian basis sets were employed. The smallest basis set $(14s10p4d1f)/[7s5p3d1f]$Na, $(15s13p4d1f)/[9s7p3d1f]$K (hereafter referred to as B-I) was obtained from the standard basis for finite-field electric property calculations [51] by decontracting the outermost d functions and adding the f functions with exponential parameters 0.06(Na) and 0.04(K). Basis II (B-II) comprised additional single sets of diffuse s, p, d, and f functions on each center. Orthogonal one-particle functions were generated by solving the state-average SCF problem for two lowest states of NaK^+. The configuration subspace spanned by all the configurations with doubly occupied core MO's (i.e., the two-valence electron CI subspace) was considered as a model space for MPPT calculations with the basis B-I. In passing to the basis B-II we restricted the model space size to $\sim$500 by omitting valence configurations with negligible contributions to the target WF's. Within the model space we have constructed a state-selective Hermitian effective Hamiltonian [48], which incorporated the core-valence correlation and the remaining core polarization effects at second order in MPPT. At the perturbation step the innermost core orbitals $1s$(Na) and $1s2s2p$(K) were kept frozen, i.e., 18 electrons were correlated explicitly.

The diagonalization of the effective Hamiltonian yielded the energy values of both states under study simultaneously. It should be emphasized that this ''diagonalization-after-perturbation'' strategy is essential for reproducing the effect of core-valence correlations on the composition of the valence part of WF's and therefore on the diffuse part of the charge-density distribution. In contradiction to the effective potential method used in [4–6], our approach takes properly into account the effective two-particle interactions of valence electrons arising from core-valence correlations. Let us finally mention that the present MPPT scheme ensures exact (for complete model spaces, basis B-I) or at least very good approximate (for restricted model spaces used with basis B-II) size consistency of the results [48]. This feature is particularly important because of the relatively large number of correlated electrons.

Let us now consider the results. The dipole moment function $d(R)$ values calculated by the finite-field MPPT with different basis sets (B-I and B-II) are presented in Table III. It may be seen that extension of the basis set from B-I to B-II almost does not affect the results in both $D\ ^1\Pi$ and $B\ ^1\Pi$

TABLE III. Finite-field MPPT results of *ab initio* dipole moment (d) calculations (in a.u.) for $B\ ^1\Pi$ and $D\ ^1\Pi$ states obtained with two atomic basis sets (B-I and B-II). Positive d value indicates Na^-K^+ polarity.

	$d(B\ ^1\Pi)$		$d(D\ ^1\Pi)$	
R (bohr)	B-I	B-II	B-I	B-II
6.0	−0.392	−0.391	1.075	1.104
7.0	−0.842	−0.831	1.944	1.929
8.0	−1.241	−1.183	2.616	2.636
9.0	−1.187	−1.164	2.731	2.787
10.0	−0.922	−0.894	2.246	2.339
11.0	−0.632	−0.608	1.558	1.655
12.0	−0.402	−0.387	0.958	1.097

states within the R range exploited. Resulting finite-field MPPT $d(v)$ functions and $d(R)$ values, along with effective potential data [4], are presented in Figs. 6 and 8 for the $D\ ^1\Pi$ state and in Figs. 9 and 10 for the $B\ ^1\Pi$ state, respectively.

Although we had no intention to study the potential curves, we found it interesting to see how the methods used here are able to reproduce the difference potential between the $D\ ^1\Pi$ and $B\ ^1\Pi$ states where the PEDM's have been calculated. The results presented in Fig. 11 show that the present MPPT calculations agree markedly better with experimental RKR values than MRCI and Ref. [4] results, thus demonstrating the correlation between the accuracy of the methods in reproducing energetic and electric properties.

VII. THE EFFECT OF $^1\Pi \sim {}^3\Pi$ SPIN-ORBIT INTERACTION

As it is well known, the singlet $D\ ^1\Pi$ and the closely lying triplet $d\ ^3\Pi$ states perturb each other owing to the spin-orbit interaction. In spite of the fact that both states are in the same energy range, their interaction is of a purely local nature, since only levels with certain v and J exhibit considerable interaction, namely the ones with sufficiently close energies and appreciable overlap integral $\langle v_s^J(D\ ^1\Pi)|v_t^J(d\ ^3\Pi)\rangle$ values [52]. If we neglect mixing between different $d\ ^3\Pi$ state Ω components $^3\Pi_{0,1,2}$, the spin-orbit interaction operator $\hat{\mathbf{H}}_{so}$ produces the only nonzero matrix elements $\langle D\ ^1\Pi|\hat{\mathbf{H}}_{so}|d\ ^3\Pi_1\rangle$. Then, vibronic WF's for perturbed levels will be expressed by a linear combination of unperturbed WF's $\Psi^0(d\ ^3\Pi_1)$ and $\Psi^0(D\ ^1\Pi)$ as $\Psi^{pert}(D\ ^1\Pi, d\ ^3\Pi_1) \approx C_s\Psi^0(D\ ^1\Pi) + C_t\Psi^0(d\ ^3\Pi_1)$, where $\Psi^0(d\ ^3\Pi_1) = \Psi^{el}(d\ ^3\Pi_1)|v_t^J\rangle, \Psi^0(D\ ^1\Pi) = \Psi^{el}(D\ ^1\Pi)|v_s^J\rangle$, and mixing coefficients C_s and C_t are normalized to unity: $C_s^2 + C_t^2 = 1$. Vibrational WF's $|v_s^J\rangle$ and $|v_t^J\rangle$, as well as adiabatic electronic WF's $\Psi^{el}(d\ ^3\Pi_1)$ and $\Psi^{el}(D\ ^1\Pi)$, are dependent on the internuclear distance R. Since L uncoupling and PEDM operators do not mix states with different multiplicity, the perturbed q factors (q^{pert}) and dipole moments (d^{pert}) can be written as a combination $q^{pert}(v,J) \approx q^0_{v_sJ} + C_t^2(q^0_{v_tJ} - q^0_{v_sJ})$ and $d^{pert}(v,J) \approx d^0_{v_sJ} + C_t^2(d^0_{v_tJ} - d^0_{v_sJ})$, where $q^0_{v_sJ}(D\ ^1\Pi), d^0_{v_sJ}(D\ ^1\Pi)$ and $q^0_{v_tJ}(d\ ^3\Pi_1), d^0_{v_tJ}(d\ ^3\Pi_1)$ are the respective values for deperturbed singlet and triplet states.

To analyze the perturbation strength for $D\ ^1\Pi$ rovibronic states involved in q and d measurements, see Table I, we have calculated the mixing coefficients C_s and C_t using deperturbed $d\ ^3\Pi$ state molecular constants, which were determined from the level shifts experimentally measured in Ref. [52] using the nondiagonal electronic spin-orbit matrix element value $\xi_{so}^{el} = 4.2 \pm 0.2\ cm^{-1}$ [52]. The overlap integrals needed to evaluate the vibronic spin-orbit matrix elements entering in $H_{so} = \xi_{so}^{el}\langle v_s|v_i\rangle$ have been calculated numerically on the basis of vibrational WF's obtained from the solution of Eq. (9) with IPA [34] and RKR [52] $D\ ^1\Pi$ and $d\ ^3\Pi$ potentials, respectively. It turned out that only two levels from Table I, namely $v_s = 11, J = 46$ and $v_s = 12, J = 7$, possess, although not very large, a considerable triplet state admixture: $C_t^2(v_t = 12, J_t = 46) \approx 0.12$ and $C_t^2(v_t = 13, J_t = 7) \approx 0.13$. Now, since the mixing coefficients C_t^2 along with the singlet-state experimental q and d values are known, and supposing that their fitting values can be taken as the deperturbed ones, we estimated the deperturbed d_t^0 and q_t^0 values: $d^0_{v_t=12,J=46} \approx (-2.0 \pm 1.1)$ D, $d^0_{v_t=13,J=7} \approx (-3.1 \pm 1.9)$ D, $q^0_{v_t=12,J=46} \approx (-1.5 \pm 0.4) \times 10^{-5}\ cm^{-1}$, and $q^0_{v_t=13,J=7} \approx (-1.6 \pm 0.5) \times 10^{-5}\ cm^{-1}$. Taking into account large relative errors in small mixing coefficients, our d_t^0 and q_t^0 estimation is by no means an accurate one. We can, however, advocate the fact that the dipole moments of the singlet and the triplet have opposite signs. Indeed, this result is in perfect agreement with the findings of *ab initio* studies. In particular, the pseudopotential calculations [4] yielded the $d\ ^3\Pi$ dipole moment value $d_t^0 = -2.3$ D for $R = 8$ a.u., the latter being close to R_e for this state. Besides, the all-electron MPPT (B-II) scheme described in Sec. VI yields the $d\ ^3\Pi$ state equilibrium dipole moment estimate $d_t^0 = -2.2$ D. It is interesting to note that the signs of the $d\ ^3\Pi$ and $D\ ^1\Pi$ state dipole moment functions coincide for $R > 9.4$ a.u. The negative sign of the $d\ ^3\Pi$ state q factors (the f component lies higher than the e component), see Fig. 1, shows unambiguously that the q values are mainly determined by interaction with the lower $c\ ^3\Sigma^+$ state. Λ doubling of the triplet Ω component $^3\Pi_1$ is caused by the interaction between f components of $^3\Pi_1$ and $^3\Sigma^+$ states [14], unlike the e-component interaction of singlet states. Now, assuming that the interacting $d\ ^3\Pi$ and $c\ ^3\Sigma^+$ states at small R can be related to the

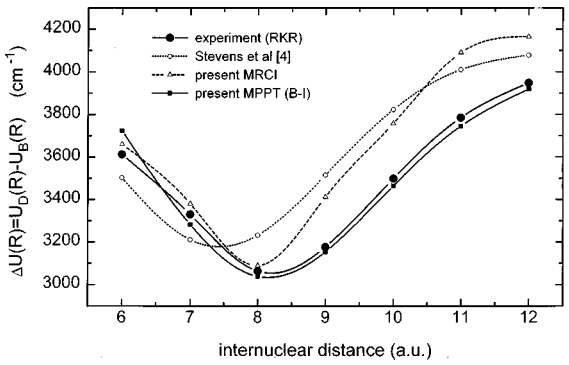

FIG. 11. Difference potential $\Delta U(R)$ between $D\ ^1\Pi$ and $B\ ^1\Pi$ states.

same $3d$-Rydberg complex [4], we arrive at the following estimate:

$$q_t^0(d\ ^3\Pi_1) \approx -\frac{2l(l+1)B_e^2(d\ ^3\Pi_1)}{T_e(d\ ^3\Pi_1)-T_e(c\ ^3\Sigma^+)} \approx -1.2\times 10^{-5}\ \text{cm}^{-1}, \quad (16)$$

where $l=2$ for the d complex.

VIII. CONCLUDING REMARKS

(i) To make definite conclusions on the behavior of Λ-doubling constants $q(v,J)$ and PEDM's $d(v,J)$ in excited states, it is necessary to perform reliable measurements in as wide as possible a v,J (or, consequently, R) range. A combination of dc Stark and RF-ODR methods in laser-induced fluorescence turned out to be adequate to achieve this aim.

(ii) The measured Λ-doubling factors $q(v,J)$ allow one to describe the specific electronic structure of a $^1\Pi$ state. In particular, it appeared to be possible to understand the principal difference between the electronic structure of the first two excited singlet $^1\Pi$ states in the NaK molecule, namely that, while the $B\ ^1\Pi$ state is essentially πp, the $D\ ^1\Pi$ one contains a considerable ($\sim$44%) πd admixture. By analyzing $^1\Pi \sim {}^1\Sigma^+$ interactions, it was possible to show that Λ doubling is caused by a single $C\ ^1\Sigma^+$ perturber in the $D\ ^1\Pi$ state, and by two competing perturbers ($A\ ^1\Sigma^+$ and $C\ ^1\Sigma^+$) in the $B\ ^1\Pi$ state.

(iii) Systematic $q(v,J)$ and $d(v,J)$ measurements make it possible to single out, by means of d and q values dropping out from a smooth variation, the local singlet-triplet interaction and, what is more, to evaluate the respective q_t and d_t values for the perturbing (dark) $d\ ^3\Pi$ state, which has not been studied directly.

(iv) The suggested inversion procedure allows us to determine reliable $d(R)$ functions from the measured $d(v,J)$ values.

(v) It was confirmed that, in order to obtain highly accurate calculated PEDM's for excited electronic states (as distinct from the ground states), one has, first, to account correctly for effective interactions of valence electrons arising from core-valence correlations. Apparently, this cannot be done properly by means of pseudopotential technique. Second, for the approximate WF's that do not strictly obey the Hellmann-Feynman theorem, it is preferable to use the finite-field strategy. The latter inclines one to think that it does make sense to apply an external electric field both in measurements and calculations.

ACKNOWLEDGMENTS

This work was supported by the European Commission in the framework of PECO Human Capital and Mobility (Network) LAMDA Programme under Contract No. ERB-CIPDCT940633, and we are especially indebted to Dr. Henrik Rudolph and Dr. Henk Dijkerman for their constant efforts in helping us to carry out the project. The Riga group participants have been supported by the Latvian Science Council (Grant No. 96.0323). Financial support of this work by the Russian Fund of Fundamental Research under Grant Nos. 96-03-32331a and 97-03-33714a is gratefully acknowledged by three of us (E.P., A.S., and A.Z.). The authors are heartily indebted to Dr. A. Shcherbinin and A. Granovskii for their help in using the GAMESS package, as well as to the investment company TERM Ltd. for granting CPU time for the MRCI calculations. A.Z. thanks Professor Björn O. Ross for supplying him with the MOLCAS 3 software. Support by the research group ''Interaction of Oriented Molecules'' of the Center for Interdisciplinary Research (ZiF) at the University of Bielefeld is gratefully acknowledged by one of us (M.A.). We are grateful to Dr. Klaus Stark for providing us with his unpublished results of NaK *ab initio* CI calculations using the MOLPRO program package. We are especially grateful to Janis Alnis for participation in the measurements. We are indebted to Dr. Jazep Eidus for his assistance in the preparation of the paper.

[1] K. P. Huber and G. Herzberg, *Molecular Spectra and Molecular Structure. IV. Constants of Diatomic Molecules* (Van Nostrand, New York, 1979).
[2] J. Derouard, H. Debontride, T. D. Nguyen, and N. Sadeghi, J. Chem. Phys. **90**, 5936 (1989).
[3] M. Tamanis, M. Auzinsh, I. Klincare, O. Nikolayeva, A. V. Stolyarov, and R. Ferber, J. Chem. Phys. **106**, 2195 (1997).
[4] W. J. Stevens, D. D. Konowalow, and L. B. Ratcliff, J. Chem. Phys. **80**, 1215 (1984).
[5] W. Müller and W. Meyer, J. Chem. Phys. **80**, 3311 (1984).
[6] S. Magnier and Ph. Millie, Phys. Rev. A **54**, 204 (1996).
[7] R. F. Wormsbecher, M. M. Hessel, and F. J. Lovas, J. Chem. Phys. **74**, 6983 (1981).
[8] K. Stark (unpublished).
[9] H.-J. Werner and P. J. Knowles, *User's Manual for* MOLPRO (University of Sussex, Brighton, 1995).
[10] H. Lefebvre-Brion and R. W. Field, *Perturbations in the Spectra of Diatomic Molecules* (Academic, New York, 1986).
[11] M. Mizushima, *Theory of Rotating Diatomic Molecules* (Wiley, New York, 1975).
[12] M. M. Hessel and S. Giraud-Cotton (unpublished).
[13] R. E. Drullinger, M. M. Hessel, and E. W. Smith, in *Laser Spectroscopy*, edited by S. Haroche *et al.* (Springer, Berlin, 1975), p. 91.
[14] H. Katô, M. Sakano, N. Yoshie, M. Baba, and K. Ishikawa, J. Chem. Phys. **93**, 2228 (1990).
[15] M. Baba, S. Tanaka, and H. Katô, J. Chem. Phys. **89**, 7049 (1989).
[16] C. A. Moore, G. P. Davis, and R. A. Gottscho, Phys. Rev. Lett. **52**, 538 (1984).
[17] R. A. Gottscho, Phys. Rev. A **36**, 2233 (1987).
[18] J. Derouard and N. Sadeghi, Opt. Commun. **57**, 239 (1986).
[19] K. Blum, *Density Matrix Theory and Application* (Plenum, New York, 1996).
[20] R. N. Zare, *Angular Momentum* (Wiley, New York, 1988).
[21] G. Herzberg, *Molecular Spectra and Molecular Structure* (Van

Nostrand, Princeton, NJ, 1957).
[22] S. J. Silvers, T. H. Bergeman, and W. Klemperer, J. Chem. Phys. **52**, 4385 (1970).
[23] J. Pfaff, M. Stock, and D. Zevgolis, Chem. Phys. Lett. **65**, 310 (1979).
[24] M. Tamanis, M. Auzinsh, I. Klincare, O. Nikolayeva, R. Ferber, A. Zaitsevskii, E. A. Pazyuk, and A. V. Stolyarov, J. Chem. Phys. (to be published).
[25] M. Auzinsh and R. Ferber, *Optical Polarization of Molecules* (Cambridge University Press, Cambridge, 1995).
[26] C. H. Townes and A. L. Shawlow, *Microwave Spectroscopy* (McGraw-Hill, New York, 1955).
[27] M. H. Alexander, P. Andresen, R. Bacis, R. Bersohn, F. J. Comes, P. J. Dagdigian, R. N. Dixon, R. W. Field, G. W. Flynn, K.-H. Gericke, E. R. Grant, B. J. Howard, J. R. Huber, D. S. King, J. L. Kinsey, K. Kleinermanns, K. Kuchitsu, A. C. Luntz, A. J. McCaffery, B. Pouilly, H. Reisler, S. Rosenwaks, E. W. Rothe, M. Shapiro, J. P. Simons, R. Vasudev, J. R. Wiesenfeld, C. Wittig, and R. N. Zare, J. Chem. Phys. **89**, 1749 (1988).
[28] K. F. Freed, J. Chem. Phys. **45**, 4214 (1966).
[29] I. I. Sobelman, *Atomic Spectra and Radiative Transitions* (Springer, Berlin, 1992).
[30] J. Bulthuis, J. M. Milan, H. M. Jassen, and S. Stolte, J. Chem. Phys. **94**, 7181 (1991).
[31] W. Gordy and R. Cooks, *Microwave Molecular Spectra* (Interscience, New York, 1979).
[32] M. W. Schmidt, K. K. Baldrige, J. A. Boatz, J. H. Jensen, S. Koseki, M. S. Gordon, K. A. Nguyen, T. L. Windus, S. J. Su, N. Matsunaga, and S. T. Elbert, J. Comput. Chem. **14**, 1347 (1993).
[33] W. M. Kosman and J. Hinze, J. Mol. Spectrosc. **56**, 93 (1975).
[34] C. R. Vidal and H. Scheingraber, J. Mol. Spectrosc. **65**, 46 (1977).
[35] R. F. Barrow, R. M. Clements, J. Derouard, N. Sadeghi, C. Effantin, J. d'Incan, and A. J. Ross, Can. J. Phys. **65**, 1154 (1987).
[36] B. R. Johnson, J. Chem. Phys. **67**, 4086 (1977).
[37] L. F. Richardson, Philos. Trans. R. Soc. London, Ser. A **226**, 299 (1927).
[38] A. V. Abarenov and A. V. Stolyarov, J. Phys. B **23**, 2419 (1990).
[39] J. H. van Vleck, Phys. Rev. **33**, 467 (1929).
[40] E. A. Colbourn and F. D. Wayne, Mol. Phys. **37**, 1755 (1979).
[41] L. B. Ratcliff, D. D. Konowalow, and W. J. Stevens, J. Mol. Spectrosc. **110**, 242 (1985).
[42] L. Lawson and R. J. Hanson, *Solving Least Squares Problems* (Prentice-Hall, Englewood Cliffs, NJ, 1974).
[43] Y. Liu, J. Li, M. Xue, D. Chen, L. Li, and G.-H. Jeng, J. Chem. Phys. **103**, 7213 (1995).
[44] A. Yiannopoulou, T. Leininger, A. M. Lyyra, and G.-H. Jeng, Int. J. Quantum Chem. **57**, 575 (1996).
[45] J. A. Pople, J. W. McIver, and N. S. Ostlund, J. Chem. Phys. **49**, 2965 (1968).
[46] A. J. Sadlej, J. Chem. Phys. **75**, 320 (1981); G. H. F. Diercksen and A. J. Sadlej, *ibid.* **75**, 1253 (1981), and references therein.
[47] P. M. Kozlowski and E. R. Davidson, Int. J. Quantum Chem. **53**, 149 (1995).
[48] A. Zaitsevskii and J. P. Malrieu, Theor. Chim. Acta **96**, 269 (1997), and references therein.
[49] R. Cimiraglia and A. Zaitsevskii (unpublished).
[50] K. Andersson, M. R. A. Blomberg, M. P. Fülscher, G. Karlström, V. Kellö, R. Lindh, P. Ä. Malmquist, J. Noga, J. Olsen, B. O. Roos, A. J. Sadlej, P. E. M. Siegbahn, M. Urban, and P. O. Wildmark, MOLCAS-3 (University of Lund, Sweden, 1995).
[51] A. J. Sadlej and M. Urban, J. Mol. Struct.: THEOCHEM **234**, 147 (1991).
[52] P. Kowalczyk, J. Mol. Spectrosc. **136**, 1 (1989).